HYDROGEN DISPERSION IN A CLOSED ENVIRONMENT

M. DE STEFANO [a,b], X. ROCOURT[b] , I. SOCHET[b], N. DAUDEY[a]
[a] EDF SEPTEN– Villeurbanne, France, nicolas.daudey@edf.fr.
[b] INSA Centre Val de Loire, Université d'Orléans, PRISME EA 4229, Bourges, France, maria.de_stefano@insa-cvl.fr, xavier.rocourt@insa-cvl.fr, isabelle.sochet@insa-cvl.fr.

Keywords: Hydrogen, Dispersion, Small Scale, Leak.

ABSTRACT

The highly combustible nature of hydrogen poses a great hazard, creating a number of problems with its safety and handling. As a part of safety studies related to the use of hydrogen in a confined environment, it is extremely important to have a good knowledge of the dispersion mechanism. The release of hydrogen may result in the formation of an explosive atmosphere, which can explode and cause serious damage.

The present work investigates the concentration field and flammability envelope from a small scale leak. The hydrogen is released into a 0.47 m x 0.33 m x 0.20 m enclosure designed as a 1/15 – scale model of a room in a nuclear facility. The performed tests evaluates the influence of the initials conditions at the leakage source on the dispersion and mixing characteristics in a confined environment. The role of the leak location and the presence of obstacles, are also analyzed. Throughout the test, during the release and the subsequent diffusion phase, temporal profiles of hydrogen concentration are measured using the thermal conductivity gauges within the enclosure. In addition, the BOS (Background Oriented Schlieren) technique is used to visualise the cloud evolution inside the enclosure. These instruments allow the observation and quantification of the stratification effects.

1. INTRODUCTION

1.1 Background

The production and consumption of hydrogen in industry is considerable, and its use as an energy carrier is particularly interesting for the future.

The highly flammable nature of hydrogen presents a great danger and poses numerous safety problems. Hydrogen has a low density (about 14 times lower than air at standard temperature and pressure) and a wide range of flammability in air (4% - 75% vol.). These features show that it could disperse quickly during an accidental release and burn easily in the presence of an ignition source. A good understanding of the dispersion and stratification of a hydrogen leak is therefore of fundamental importance in order to better understand the possibility of ignition and explosion of accidental releases.

This article deals with the analysis of the risks associated with a hydrogen leak in a nuclear power plant. It presents experimental tests to characterize hydrogen dispersion in an enclosure under non-ventilation conditions. In order to facilitate testing and limit the amount of gas, a 1/15 scale enclosure of the represented room of a nuclear facility has been adopted. The simple geometry of the enclosure make it possible to use the results also in general cases of physical flow behaviour. A dense mesh of instrumentation is used to better understand how hydrogen behaves when it is released in a confined space and especially to assess under what circumstances explosive mixtures can develop.

The purpose of this study is twofold. First, it consists of experimentally characterizing the hydrogen dispersion according to various parameters such as the flow and the leakage position. Second, it provides a set of reference data to test and validate the ability of CFD codes to predict concentrations and distributions in an enclosure.

1.2 Previous work

Over the past decade, many studies have been devoted to the understanding of the dispersion of hydrogen in an enclosed space, experimentally and numerically through CFD codes.

The studies mentioned below were carried out under various conditions such as confined or unconfined, large or small scale, with or without ventilation. The behaviour of the dispersion of hydrogen depends, in fact, on many factors such as: the discharge conditions (flow, pressure, location and direction), the geometry of the enclosure (size and shape of the enclosure, openings, presence of obstacles), and atmospheric conditions inside and outside the enclosure. Experiments with helium are included as it can be used as a substitute to study the phenomena of hydrogen dispersion for safety reasons. Although the density of helium is twice that of hydrogen, its use is justified at low concentrations [1]. In addition, the tests performed by Swain et al. [2] showed a strong similarity between helium and hydrogen. They studied the differences between the emissions of two gases using a CFD approach, it is validated by experimental measurements of helium.

Denisenko et al. [3] analysed the mechanisms and kinetics of the evolution of hydrogen clouds in confined spaces of different shapes and sizes and different release conditions. Hydrogen was released in a small scale container (4 m^3) and in a room with a volume of 25 m^3. Moreover, they have also diffused helium at different velocity in a garage-sized room in order to better understand the role of the flow rate in the distribution of the cloud. The results show that for a given flow rate, it is possible to distinguish two different types of dispersions of the cloud in a confined enclosure. In their first case, where a low flow rate is maintained, the cloud initially forms in the shape of a layer on the ceiling and then expands downwards. In the second case, where a high flow rate is maintained, the cloud disperses almost uniformly throughout the volume above the discharge point.

Denisenko [3] characterized the difference between the two cases by the value of Morton $M = l_s/z$ where l_s is the momentum length scale $\left(l_s = \frac{M_0^{3/4}}{F_0^{1/2}}\right)$ and z the distance between the point of release and the ceiling. According to the experimental data, for situations where $M < 1$, there is a stratification of the concentration of hydrogen, whereas for $M >> 1$, a homogenization is observed throughout the room.

Gupta et al. [4] studied the concentration distributions caused by the dispersion of helium in a chamber representing a residential garage (5.76 x 2.96 x 2.42 m^3). The room was equipped with small openings near the base to minimize pressure differences between the interior and exterior of the enclosure, while limiting the loss of the injected gas. They performed four tests based on flow, velocity and injected volume. In all the tests, the cloud formed laminated layers inside the facility. Analysis of the results clearly indicates that the risk of inflammation is highly dependent on the total volume injected rather than the flow rate. Test cases with similar injected gas volumes but different initial conditions (flow rate and injection rate), at the end of the injection phase, show a nearly identical maximum concentration. Subsequent work in the same facility was conducted by Cariteau et al. [5] for studying the effects of exit velocity and vent location on the helium dispersion. The vertical distribution of the volume fraction was analysed for three different ventilation conditions: zero ventilation, vent at the bottom of the room and vent at the top of the room. In the third configuration, the exchange rate with the outside was much higher than in the other cases and consequently the presence of the vent led to reducing the flammable volume. In the case of zero ventilation, the spatial and temporal variations of the volume fraction are in good agreement with the theoretical model of Worster and Huppert [6]. Moreover, Cariteau [5] found that stratification occurs over a wide range of flow rates independently of the opening position. Opening at the ceiling promotes mixing but not enough to produce a homogeneous mixture. Cariteau [7] also studied the dispersion of helium in a small-scale chamber (0.93 x 0.93 x 1.26 m^3). The formation of the stratified layers as a function of the Richardson number (Ri) was examined. The results of these experiments give a clear identification of the three filling regimes: stratified regime, stratified regime with a homogeneous layer and homogeneous regime. For values of the Richardson Ri number greater than unity, it is possible to find a regular stratification similar to that provided by the one-dimensional model of Worster and Huppert [6]. The transition is realized from a number of Ri less than one and the homogeneous regime is verified when the approximate value of Ri ~ 0.0032. Some of the data presented by Cariteau [7] were used for the validation of CFD codes [8].

Pitts et al. [9] conducted a series of helium dispersion tests in an enclosure measuring 1.5 x 1.5 x 0.75 m^3, which is equivalent to the size of ¼ of a residential garage. They characterized the effects of the location of the gas leak and various sizes and locations of vents on the evolution of concentration profiles during release and post-release periods. Eighteen combinations were studied with two leakage times, three leak positions (center down, center up and on the side) and three vent configurations. Comparison of average concentration values for experiments with individual vent in the centre of the front wall, have

revealed that the dispersion is not much affected by leak position, release time, and vent size. With two vents, one located near the floor and the other on the ceiling, the average concentration of helium at the end of a discharge is greatly reduced compared to experiments with a single large vent of a similar total ventilation area. These observations indicate that significant amount of air have entered the garage during the release phase. The increase in air infiltration is due to the relatively large pressure difference between the inside and the outside and the lower density fluid inside the garage. The use of these data to validate CFD codes has been described in the work of Prasad et al. [10] who used the data from this study to confirm the ability of the CFD code of the NIST FDS to predict helium distributions.
One of the most important studies for using data as a basis for CFD codes is that of Lacome et al. [11]. They studied the spatial and temporal distribution of hydrogen released inside a cave (7.2 x 3.78 x 2.88 m^3) representing a garage with a single vent near the floor. The study parameters were the flow rate and the duration of injection. The experimental results show that for the cases studied, a clear stratification of a mixture of more or less rich hydrogen can be observed in the upper part of the room. If the duration of injection increases, the layer becomes thicker but its concentration remains relatively homogeneous and constant over time.
One of the tests described by Lacome et al. [11] was the basis for a study led by Venatostos et al. [12] on CFD codes capacity. The calculations were performed prior to the availability of the experimental results and then repeated thereafter. In the blind test, there are significant differences between the experimental measurements of hydrogen concentration and the predicted values of the CFD codes. The most important differences are the sensors located in the lower part. Differences between experimental concentrations and those calculated through codes were reduced after experimental data was available, but discrepancies remain.
Another interesting study for modelling the dispersion of hydrogen with a variety of CFD codes was made by Gallego et al. [13], in collaboration with 12 laboratories by using database of Shebeko et al. [14]. The experiment was carried out inside a cylindrical vessel of 20 m^3 volume. The concentration of hydrogen was measured at 6 points along the axis after the release phase for a period of 250 minutes. These numerical studies have led to the conclusion that CFD models can provide reasonable agreement with experimental data.

2. EXPERIMENTAL SETUP

2.1 Instrumentation

The experimental facility represents a 1/15 - scale model of a room of a nuclear facility. In order to carry out general and non-specific cases, the location taken as a reference is a simple room of a nuclear facility which contains line portions of the hydrogen, where leakage can occur, also there may be several obstacles.The model used is a rectangular enclosure with internal dimensions of 0.47 x 0.33 x 0.20 m^3 length, width and height respectively (Fig. 1).

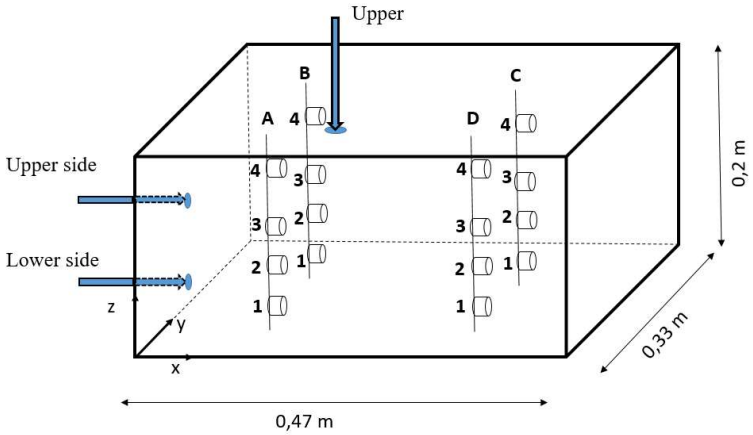

Figure 1. Experimental enclosure scheme and sensor positions.

The enclosure is equipped with a pressure sensor to control the internal pressure. An air and nitrogen sweep is carried out at the end of the procedure allowing the experimental enclosure to be inerted.
Hydrogen and nitrogen are injected into the room through a solenoid valve system. Flow rates at the nozzle exit are measured and controlled with two mass flow controllers (BROOKS). Both controllers can provide accurate flow rates over a range of 0 to 6 $Nm^3 \cdot h^{-1}$, with uncertainties of ± 0.9% on the full scale. The response time of the flux output signals for the flowmeters is less than 2 s.
The hydrogen concentrations are measured using XEN-5320 (Xensor) catharometers. Their small dimensions (sensor diameter d = 0.005 m) and their data rate (3 Hz) make it possible to measure the concentration pointwise every 0.33 s. For an extended concentration measurement, 16 sensors are used inside the installation. They are fixed on four rods, denoted as A, B, C and D in figure 1, with four sensors on each, so as to cover the entire volume. Table 1 summarizes the location of the sensors.

Table 1. Positions of the concentration sensors.

Rod	Position	x (m)	y (m)	z (m)
A	1	0.13	0.07	0.04
	2	0.13	0.07	0.08
	3	0.13	0.07	0.12
	4	0.13	0.07	0.18
B	1	0.13	0.24	0.04
	2	0.13	0.24	0.08
	3	0.13	0.24	0.12
	4	0.13	0.24	0.18
C	1	0.38	0.24	0.04
	2	0.38	0.24	0.08
	3	0.38	0.24	0.12
	4	0.38	0.24	0.18
D	1	0.38	0.07	0.04
	2	0.38	0.07	0.08
	3	0.38	0.07	0.12
	4	0.38	0.07	0.18

The concentration measurements were coupled with visualization. The BOS technique (Background Oriented Schlieren) was used at the jet exit. This method consists of recording a patterned image placed behind the enclosure. In this case the image consists of black square points printed on a white paper sheet. It is first recorded before the beginning of the injection, thus giving an undisturbed reference image. Then, during the release, changes of refractive index in the air / hydrogen mixture are responsible for an apparent deformation of the pattern. The subtraction of the background image from the distorted image allows to see the optical displacement of the pattern. The result is a visualization of the density gradient. Dalziel et al. [15] described this method in detail. The images were recorded at the start of the injection with a Phantom VEO 410L high-speed camera with 2000 fps (frame per second) and a resolution of 1024 x 504 pixels.

2.2 Test Scenarios

In order to understand the hydrogen dispersion and the behavior of the mixture inside the enclosure, nine test cases are studied with three flow rates for three leakage positions (Fig. 1).
The tests have been carried out in a configuration of free volume, without obstacles and without ventilation, at ambient conditions of temperature and pressure. The outlet diameter d = 0.004 m and the volume injected V = 1.55 L, 5% of the enclosure volume, are the defined parameters for all tests. The concentration of hydrogen was measured during the injection phase and then during the diffusion phase for a period of 180 seconds. The three flow rates were chosen in order to study several flow regimes according to different Reynolds numbers, defined by the relation:

$$Re = \frac{\rho_{H2} \cdot u_0 \cdot D}{\mu_{H2}}, \quad (1)$$

where ρ – density of hydrogen, kg·m^{-3}; u_0 – exit velocity, m·s^{-1}; D – diameter of the leak, m ; μ – the dynamic viscosity of the fluid, Pa·s.

The tests cover the three types of regimes: laminar flow (Re <1000), transitional flow (1000< Re < 4000) and turbulent flow (Re > 4000).

Table 2 summarizes the parameters for the test cases studied. The coordinates are given in relation to an origin located on the ground at the front of the enclosure on the left edge (Fig. 1).

Table 2. Tests cases for hydrogen releases.

Reference Flow	Q_1			Q_2			Q_3		
Reference Position	Upper	Upper side	Lower side	Upper	Upper side	Lower side	Upper	Upper side	Lower side
x release [m]	0.17	0	0	0.17	0	0	0.17	0	0
y release [m]	0.165	0.165	0.165	0.165	0.165	0.165	0.165	0.165	0.165
z release [m]	0.2	0.13	0.01	0.2	0.13	0.01	0.2	0.13	0.01
Release direction	-z	x	x	-z	x	x	-z	x	x
Volumetric flow rate [Nm^3·h^{-1}]	5.4			1.8			0.1		
Release duration [s]	1			3			46		
Re	4500			1500			83		
Ri	$1.27 \cdot 10^{-6}$			$1.14 \cdot 10^{-5}$			$3.70 \cdot 10^{-3}$		
l_s [m]	2.41			0.8			0.045		

A flow with an inertial force that initially behaves like a jet near the nozzle outlet, can behave like a pure plume in the far field. The distance l_s, beyond which the initial specific momentum $M_0 = Q_0 \cdot u_0$ [m^4·s^{-2}] becomes negligible compared to the buoyancy fluxes $F_0 = (Q_0\, g\, \Delta\rho) \cdot (\rho_{air})^{-1}$ [m^4·s^{-3}], it is called the momentum length scale and it can be estimated from equation (2) [4], as below:

$$l_s = \frac{M_0^{3/4}}{F_0^{1/2}} = \frac{0.96 \cdot u_0 \cdot \sqrt{D}}{\sqrt{\frac{g \cdot (\rho_{air} - \rho_{H_2})}{\rho_{air}}}}, \quad (2)$$

where u_0 – exit velocity, m·s^{-1}; D – diameter of the leak, m; g – acceleration of gravity, m·s^{-2}; ρ_{air} – density of air, kg .m^{-3}; ρ_{H2} – density of hydrogen, kg·m^{-3}.

The distance l_s is 2.41 m and 0.8 m for the Q_1 and Q_2 tests, respectively. It is greater than the largest dimension of the enclosure which is equal to 0.47 m. For these two test cases the flow structure is of the jet type in the enclosure for both the vertical leak and the horizontal leak. Differently, in the case of Q_3, the distance l_s is equal to 0.045 m, so the flow similar to a plume develops near the exit regardless of the direction of release (vertical or horizontal).

Each case was repeated 5 times to test the consistency of the results. The tests were compared with each other through a detailed analysis. For each sensor, the maximum concentration, ten different concentrations (t = 1 s, 2 s, 3 s, 4 s, 5 s, 10 s, 20 s, 40 s, 50 s, 80 s) and the slopes, in two different time intervals Δt_1 = (40 s - 20 s) and Δt_2 = (90 s - 60 s), of the concentration curves were compared. The results of the comparisons show that the mean relative standard deviation for the ten concentrations is less than 10% for all tests with a minimum of 7%. For the maximum concentration, the average relative standard deviation was 12% for the entry from the ceiling with flow rate Q_2 and 0.6% for the low side leak with Q_3 flow. The comparison of the slopes on the time intervals Δt_1 and Δt_2 shows an average relative standard deviation included between 1% and 18% where the highest differences are visible for the flow rate Q_1, whereas, there are lower differences in respect to the flowrate Q_3. This difference is explained by the fact that the turbulence is heavily present in the case of the flow rate Q_1 and prevents having optimum consistency. In conclusion, the tests are comparable to each other and it is possible to average the 5 tests in order to analyze the results.

3. EXPERIMENTAL RESULTATS AND DISCUSSION

3.1 Dependence of leakage flow

In this section, the influence of the flow on the concentration of hydrogen was studied for the case of leakage from the top of the enclosure. The three flows tested represent the three types of flow regimes: the turbulent flow for Q_1, the transitional flow for Q_2 and Q_3 for the laminar flow. The concentration profile of hydrogen in the enclosure with respect to time during the release and the post-release, and an image of the leak at t = 1 s, are shown in figure 2 for the three test cases.

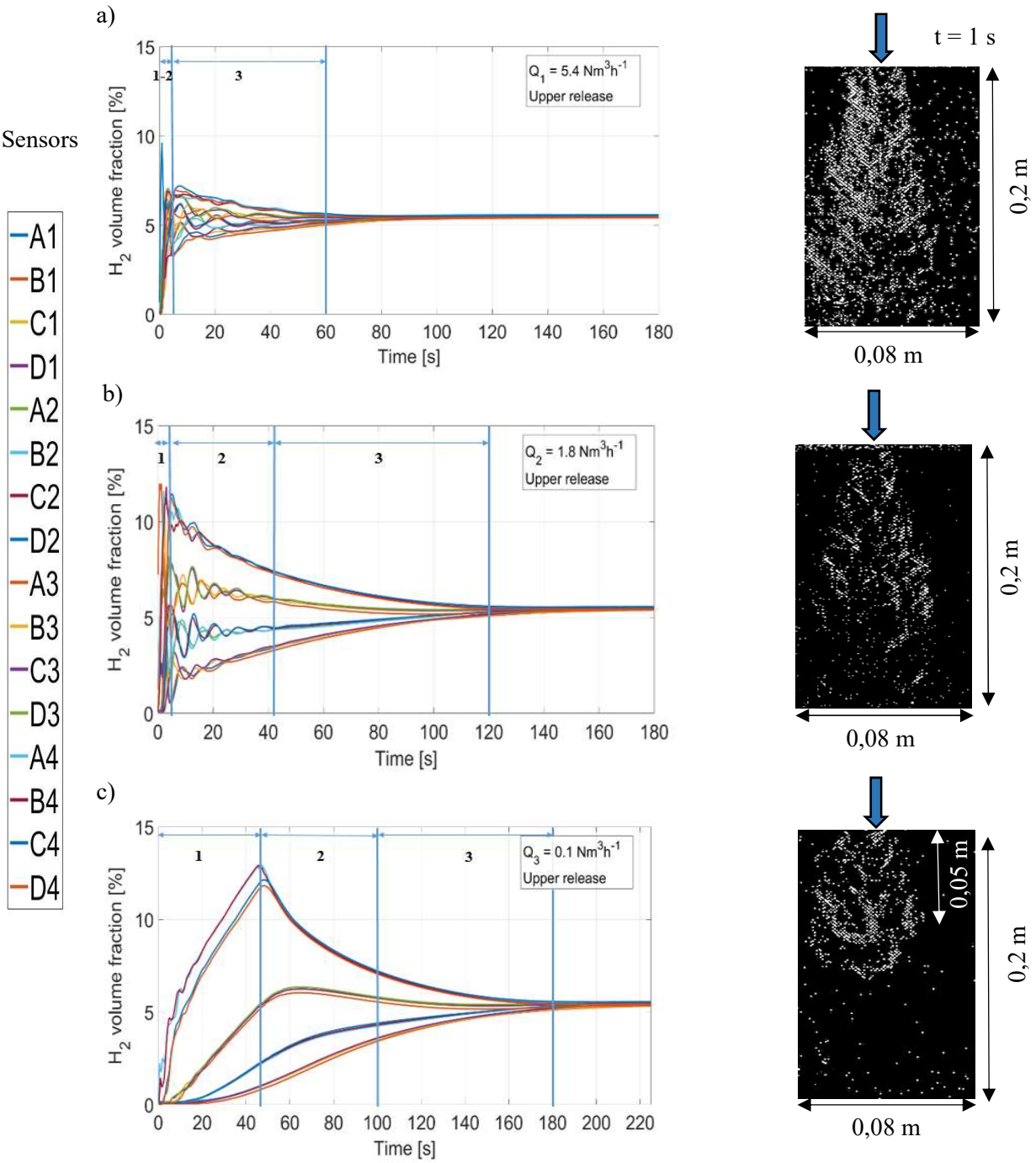

Figure 2. Volume fraction of hydrogen in function of time during the injection and dispersion phases for the 16 sensors, and images obtained at t = 1 s - Leakage from the top - flow rates: a) Q_1 = 5.4 Nm^3·h^{-1}, b) Q_2 = 1.8 Nm^3·h^{-1} and c) Q_3 = 0.1 Nm^3·h^{-1}.

By analyzing the hydrogen concentration profile as a function of time for all the tests, it is possible to divide the dispersion into three phases: injection, diffusion and mixing. In the initial phase (injection), the concentration of hydrogen increases immediately, which may be the result of the presence of inertial forces. Peak levels of concentration of hydrogen are detected by the sensors near the ceiling due to buoyancy. The intermediate phase (diffusion) following the end of the gas injection, shows that the highest concentrations layers are formed near the ceiling. In this phase, forces induced by inertia begin to decrease and the buoyancy begin to dominate the flux. During this phase, it is possible to observe vertical layers well defined in the enclosure. Once the hydrogen injection is stopped, the concentration become homogenous for all tests during the last phase. Although each test case consists of the same stages, the concentration profiles are different from each other. In the turbulent case, where $Q_1 = 5.4\ Nm^3 \cdot h^{-1}$, the first two phases last only a few seconds and the mixing takes place very quickly. Hydrogen reaches the ground more rapidly thanks to momentum-dominated forces and allows very rapid homogenization at t = 60 s. In the second case, with $Q_2 = 1.8\ Nm^3 \cdot h^{-1}$, homogenization is slower and is reached at t = 120 s (twice the time observed in the first case). Due to the lower kinetic energy, it is possible to distinguish stratification in the enclosure due to the buoyancy. In the laminar case, for $Q_3 = 0.1\ Nm^3 \cdot h^{-1}$, the jet does not reach the ground. The inertial forces are too small as compared to the buoyancy that dominate the flow from 0.05 m after the exit, as can be seen in the associated image (Fig. 2c). The mixing is slow, the homogenization is reached at t = 140 s after the end of the injection phase, and it occurs mainly because of the molecular diffusion. Consequently, a large gradient of concentration appears, and layers are formed as a function of the height, before the homogenization of the mixture with time. The levels of concentration in the upper half of the enclosure decrease, while they increase at the same time in the lower half. Significant differences between the three cases are evident for the maximum concentration reached and for the concentration gradient. In the turbulent case (Q_1) the concentration reached is 7% vol. and the gradient at the end of the injection phase t = 1 s is between 2% vol. and 7% vol.. For the laminar case (Q_3) the maximum concentration is 12.5% vol. and the gradient at t = 46 s (end of injection) is between 2% and 12%.
In all the tests cases, the hydrogen concentration levels exceed the lower limit of flammability, equal to 4% vol., and therefore the risk of explosion is present.
It is important to note that for all tests the variations in the volume fraction of hydrogen are much greater in the vertical plane than in the horizontal plane. The results of the comparisons between the sensors at the same height show that the average of relative standard deviation for concentrations is less than 5% for all tests.

3.2 Dependence of the leakage position associated with different flow rates

In order to analyze the effects of location and flow rate on the hydrogen dispersion, the comparison of the tests is carried out on three characteristics: the maximum concentration, the time to reach the homogeneous concentration after the end of the injection and the slope of the concentration curve in a defined time interval.
Since the sensors placed at the same height z on the different rods have minimal differences in concentration values, the average of the four curves of the hydrogen volume fraction was made to represent the z planes of the sensors. The comparison of the three characteristics is done as a function of z, so as to have only four points for each case studied, which represent the different heights of the sensors. The slope of the concentration curves as a function of time was calculated assuming, over a short period of time, that the curve could be represented by a straight line. In order to minimize this approximation, the time period chosen is 20 s, from t = 20 s to t = 40 s, after the end of the injection. It is important to note that for the calculation of the homogenization time and the slope, only the concentrations obtained during the diffusion phase were used, whereas the injection phase was taken into account for the calculation of the maximum concentration.
The maximum concentrations as a function of the height z for the nine cases studied (3 flow rates for 3 injection positions) are shown in figure 3. The cases having the same flow rate are represented with the same color, while the type of line changes for the different input positions.

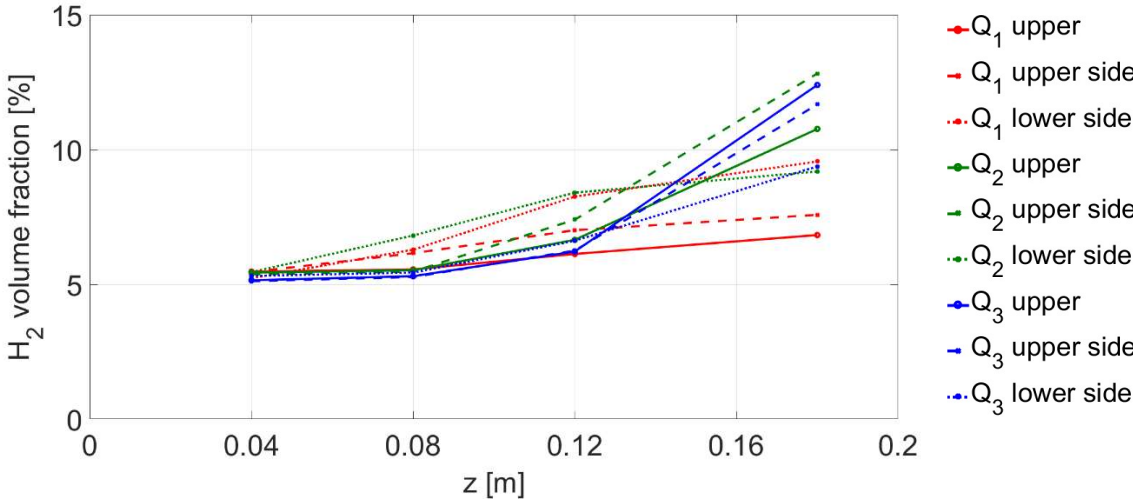

Figure 3. Maximum hydrogen volume fraction versus height z for 3 injection positions (upper, upper side, lower side) and the 3 study flows (Q_1, Q_2, Q_3).

From the analysis of figure 3, it is possible to note that the maximum concentration increases with the height for all cases due to the buoyancy of the hydrogen, it results in large accumulation of hydrogen near the ceiling. For height z = 0.04 m the maximum concentrations are the same for all cases, while for z = 0.18 m the range of values is wider. Increase in height resulting in more scattered value of hydrogen concentration in all test cases. It is possible to notice that for z = 0.18 m, the concentration values obtained for the top and top lateral leak locations are similar. The concentration values obtained for the lower side position are distinguished from the others because they are virtually independent of the leakage rate. This is because, for a low flow leak, when the leak is in the lower lateral location, the hydrogen first disperses downwards, while at other locations it immediately rises to the ceiling and reaches the ground only in the last phase (mixing phase). In order to confirm this, the maximum concentrations for the lower heights are greater in the case of lower lateral leaks. As regards the influence of the flow rate, as seen above (Fig. 2), the maximum concentration increases with the decrease of the flow rate for the three locations of the leak.
The time, required to reach the homogeneous concentration in the enclosure after the end of the injection for the nine cases studied, is shown in figure 4.

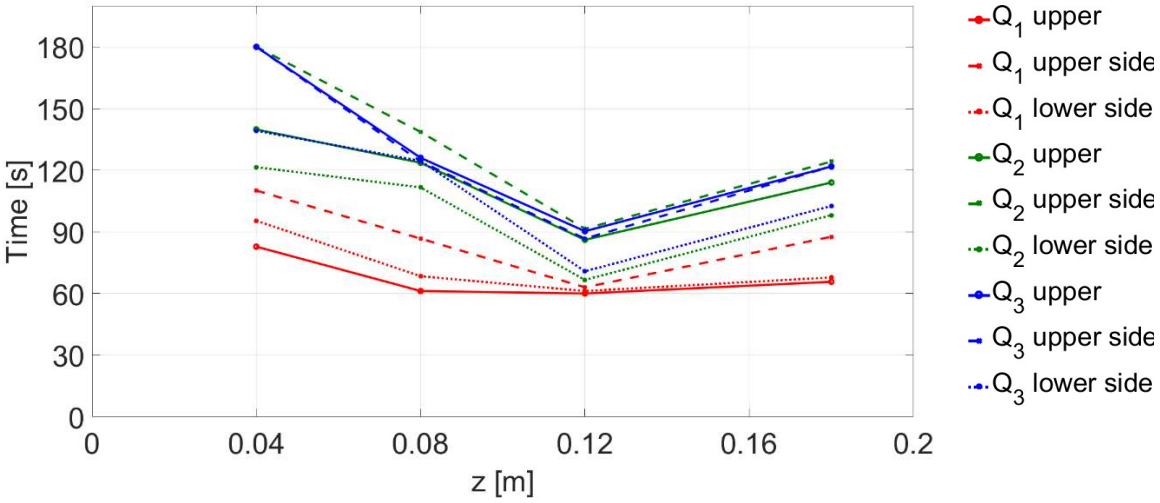

Figure 4. Time to reach the homogeneous concentration inside the enclosure after the end of the injection as a function of the height for the 3 injection positions (upper, upper side, lower side) and the 3 study flows (Q_1, Q_2, Q_3).

By comparing the results obtained for the homogenization time after the leak at the different heights, it is noteworthy in all cases that the duration is minimal for z = 0.12 m, while the maximum duration is obtained for z = 0.04 m. This means that for the sensors at the bottom, the homogeneous concentration is reached last regardless of the flow rate and the injection position. On the contrary, for the sensors located at z = 0.12 m, the homogeneous concentration is reached more rapidly. For other heights, the times are similar. As regards the influence of flow, it can be deduced from the graph (Fig. 4) that the homogenization times for all heights and locations increase if the flow rate decreases. This is due to the reduction of the kinetic energy and therefore due to the reduction of the mixing speed. At low flow rates, in the mixing phase, the buoyancy forces dominate the flow relative to the forces induced by the momentum and therefore the phenomenon is slower. When the flow rate increases, it is important to highlight a flattening of the homogenization time curve. This is due to the increase in turbulence and the decrease in the concentration gradient in cases of high flow. The influence of the leakage position is not easy to analyze because if in case of flow rate Q_1 the three curves for different locations are very close, they dissociate in case of flow rates Q_2 and Q_3. Indeed, in the case Q_2 and Q_3 the curves cross each other for the different positions of leak. For the flow Q_1, the smallest homogenization times are achieved with the leak from ceiling, because the distance between the ceiling and the floor is less than the distance between the two side walls and therefore the mixing is faster. For flow rates Q_2 and Q_3, it can be noted that the homogenization time is shorter when the leakage position is on the lower side, while the homogenization time is longest for Q_2 when the leakage is positioned on the upper side.
The values of the slopes of the concentration curves after the end of the injection for the time interval Δt = (40 s - 20 s) are shown in the figure below (Fig. 5) for the 3 positions and the 3 leakage rates.

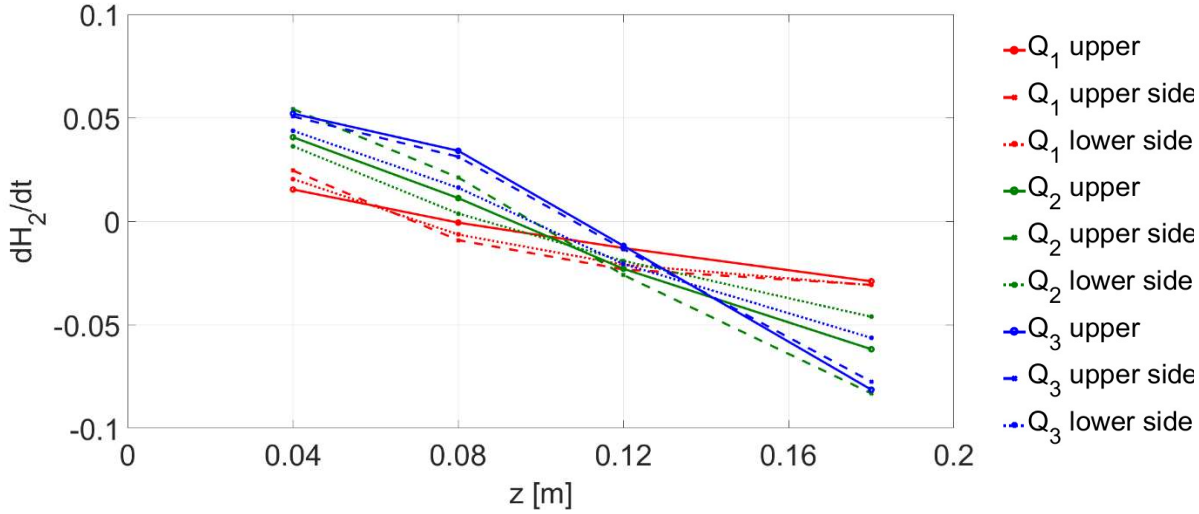

Figure 5. Slopes of the volumetric fraction of hydrogen after the end of the injection in the time interval Δt = (40 s - 20 s) as a function of the height z for the 3 injection positions (upper, upper side, lower side) and the 3 study flows (Q_1, Q_2, Q_3).

The graph, figure 5, shows that the slope sign changes as a function of height. This is due to differences between the concentration curves of the sensors on the upper half and on the lower half of the enclosure. As seen in figure 2, during the post-liberation phase, the hydrogen accumulated at the top of the enclosure migrates downwards where the concentration increases until it reaches the homogeneous concentration. At the homogenization time, the slope decreases in absolute values with the increase in flow. Since the concentration gradient is lower in a turbulent flow, the homogenization is much faster. It is also important to note that the slope does not depend on the leak position and that all the curves of the same flow rate are very close to one another.

3.3 Dependency of Obstacles

In order to analyze the hydrogen dispersion in presence of obstacles, a bar with a diameter of 0.01 m and a length of 0.47 m was positioned horizontally along the x-axis in the enclosure at z = 0.18 m and y = 0.165 m. This means that the jet at the top of the enclosure impacts the obstacle after 0.02 m. The figure below (Fig. 6) shows the comparison between the hydrogen concentration curves versus time for a leak positioned on the ceiling in the case of an empty space and the same in the presence of an obstacle, for a flow rate of $Q_1 = 5.4\ Nm^3 \cdot h^{-1}$.

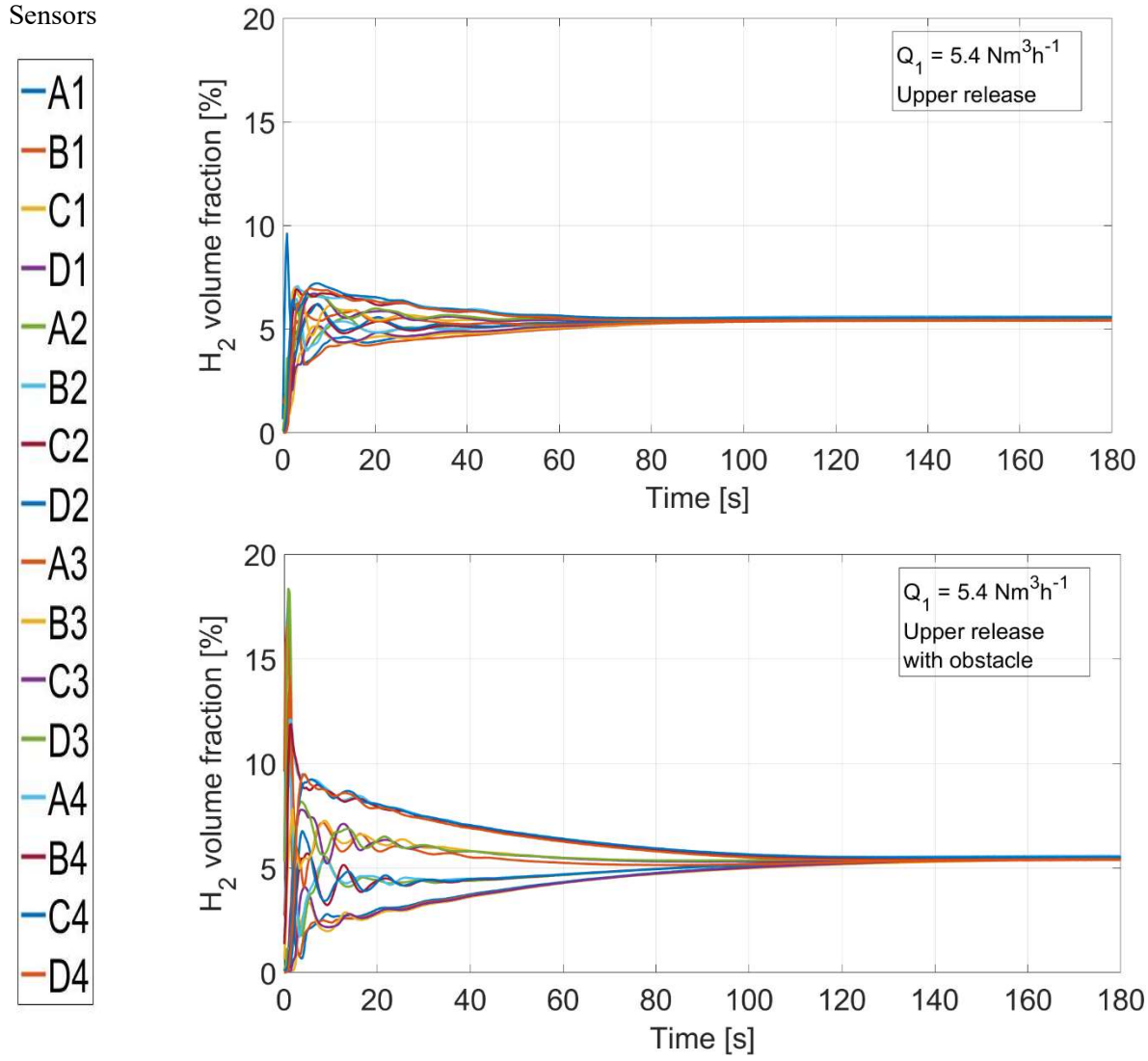

Figure 6. Comparison between the curves of the volumetric fraction of hydrogen in function of time during the injection and dispersion phase (t = 180 s) for the 16 sensors for leakage from the top with the flow rate $Q_1 = 5.4\ Nm^3 \cdot h^{-1}$ into the empty local (top) and in the local with obstacles (bottom).

It is important to note that in the case of the jet impacting an obstacle, the concentration gradients are higher. By way of example, in the empty room the concentrations at t = 20 s vary between 4.2% vol. and 6.5% vol., while in the local with the obstacles the concentration varies between 3% vol. and 8% vol. As a consequence, the time required for hydrogen to homogenize in the room is twice as large in the case of the room with obstacles (t = 120 s) than in the case of the empty space (t = 60 s). The tests also differ in the maximum concentration achieved, since in the case of empty local, c_{max} = 9.8% vol. while

in the room with the obstacle, c_{max} = 18.2% vol.. The presence of obstacles therefore has a strong impact on hydrogen dispersion and it cannot be overlooked.

4. CONCLUSION

In this article, the influence of the hydrogen dispersion in relation to the leak flow rate and location of the leak is analyzed in a small-scale enclosure. The volume fraction is measured at ambient temperature and pressure during the release and post-release phase by use of concentration sensors and video capture by the BOS method. Nine combinations of flow and leak position were studied to provide useful information to understand how hydrogen disperses.

For a given leak position, the different flow rates create significant differences for the concentrations observed between the turbulent flow, Q_1, and the laminar flow, Q_3. By analyzing the concentration curves as a function of time, it can be concluded that the higher the flow rate, the faster the hydrogen is dispersed homogeneously in the room. At high flow rate, the kinetic energy dominates the dispersion phenomenon and the hydrogen moves along the periphery of the enclosure until it fills homogeneously. When the flow rate decreases, the dispersion phenomenon is controlled by the buoyancy forces due to the density difference between the hydrogen and the air. Hydrogen, therefore, rises towards the ceiling and forms layers of different concentrations (stratification). The concentration gradients developed during the injection phase dissipate very slowly during the successive phases due to the phenomenon of diffusion. The differences between the two regimes, laminar and turbulent, result in an increase in the maximum concentration, concentration gradients and the time required to homogenize the mixture in the enclosure if the flow rate decreases.

The dispersion depends much more on the flow rate than on the position of the leak. Indeed, the differences between the different positions depend on the flow, the significance of the deviation change in position decreases with the increase in the flow. For a small flow rate it is possible to notice that the hydrogen disperses first at the bottom in the case of lower leakage and it ascends immediately to the ceiling and only goes down to the mixing phase for the other positions.

In the presence of obstacles, the results of the tests make it possible to conclude that if the jet meets an obstacle, the dispersion mechanism changes. The leak, which in the model with the empty space is controlled by the amount of motion, loses its energy when it impacts the obstacle. Hydrogen, therefore, rises to the ceiling forming higher concentration gradients and therefore has a slower homogenization time.

The experimental results presented in this paper aim to better predict the dispersion of hydrogen in confined spaces.

Some of the data presented will be used subsequently to validate the calculations carried out with the FLACS code, in order to predict the scenarios of large scale accidental release of hydrogen. This work will be extended with additional test cases to study the effects of flow and leakage orientations with obstacles, in order to be as representative as possible on a small scale inside a real local EDF. In addition to the concentration measurements, speed and turbulence measurements will also be carried out using the particle imaging velocimetry (PIV) technique for precise definition of an explosive atmosphere.

REFERENCES

1. Agranat, V., Cheng, Z. and Tchouvelev, A., CFD Modeling of Hydrogen Releases and Dispersion in Hydrogen Energy Station, Proceeding of 15th World Hydrogen Energy Conference, 27 June – 2 July 2004, Yokohama, Japan.
2. Swain, M.R., Shriber, J. and Swain, M.N., Comparisons of hydrogen, natural gas, liquidfied petroleum gas, and gasoline leakage in a residential garage, *Energy Fuels*, **12**, 1998, pp.83-89.
3. Denisenko, V., Kirillov, I., Korobtsev, S. and Nikolaev, I., Hydrogen-air explosive envelope behaviour in confined space at different leak velocities, Proceedings of 3nd International Conference on Hydrogen Safety, 16-18 September 2009, Ajaccio, France.
4. Gupta, S., Brinster, J., Studer, E. and Tkatchenko, I., Hydrogen related risks within a private garage: Concentration measurements in a realistic full-scale experimental facility, *International Journal of Hydrogen Energy*, **34**, 2009, pp. 5902-5911.

5. Cariteau, B., Brinster, J. and Tkatschenko, I., Experiments on the distribution of concentration due to buoyant gas low flow rate release in an enclosure, *International Journal of Hydrogen Energy*, **36**, 2011, pp. 2505-2512.
6. Worster, M. and Huppert, H., Time-dependent density profiles in a filling box, *Journal of Fluid Mechanics*,**132**, 1983, pp. 457-466.
7. Cariteau, B. and Tkatschenko, I., Experimental study of the concentration build-up regimes in an enclosure without ventilation, *International Journal of Hydrogen Energy*, **37**, 2012, pp. 17400-17408.
8. Bernard-Michel, G. and Cariteau, B., Helium release in a closed enclosure: comparison between simple models, CFD calculations and experimental results, Proceedings of 4th International Conference on Hydrogen Safety, 15-17 September 2011, San Francisco, USA.
9. Pitts, W.M., Yang, J.C. and Fernandez, M.G., Helium dispersion following release in a ¼ scale two car residential garage, *International Journal of Hydrogen Energy*, **37**, 2012, pp. 5286-5298.
10. Prasad, K., Pitts, W.M. and Yang, J.C., A numerical study of the release and dispersion of a buoyant gas in partially confined spaces*, International Journal of Hydrogen Energy*, **36**, 2011, pp. 5200-5210.
11. Lacome, J.M., Dagba, Y., Jamois, D., Perrette, L. and Proust, C.H., Large scale hydrogen release in an isothermal confined area, Proceedings of 2nd International Conference on Hydrogen Safety, 11-13 September 2007, San Sebastian, Spain.
12. Venetsanos, E., Papanikolaou, E., Delichatsios, M., Garcia, J., Hansen, O. R., Heitsch, M., et al., An intercomparison exercise on the capabilities of CFD models to predict the short and long term distribution and mixing of hydrogen in a garage, *International Journal of Hydrogen Energy*, **34**, 2009, pp. 5912-5923.
13. Gallego, E., Migoya, E., Martin-Valdepenas, J.M., Crespo, A., Garcia, J. and Venetsanos, A., An intercomparison exercise on the capabilities of CFD models to predict distribution and mixing of H2 in a closed vessel, *International Journal of Hydrogen Energy*, **32**, 2007, pp. 2235-2245.
14. Shebeko, Y.N., Keller, V.D., Yeremenko, O.Y., Smolin, I.M., Serkin, M.A. and Korolchenko, A.Y., Regularities of formation and combustion of local hydrogen-air mixtures in a large volume, *Chemistry & Industry*, **24**, 1988, pp. 728-731 [in Russian].
15. Dalziel, S.B., Hughes, G.O. and Sutherland, B.R.., Whole-field density measurements by 'synthetic schlieren', *Experiments in Fluids*, **28**, 2000, pp. 322-323.